Fluid Mechanics
2020; 6(1): 1-14
http://www.sciencepublishinggroup.com/j/fm
doi: 10.11648/j.fm.20200601.11
ISSN: 2575-1808 (Print); ISSN: 2575-1816 (Online)

Quinn's Law of Fluid Dynamics: Supplement #1 Nikuradze's Inflection Profile Revisited

Hubert Michael Quinn

Department of Research and Development, the Wrangler Group LLC, Brighton, USA

Email address:
hubert@wranglergroup.com

To cite this article:
Hubert Michael Quinn. Quinn's Law of Fluid Dynamics: Supplement #1 Nikuradze's Inflection Profile Revisited. *Fluid Mechanics*. Vol. 6, No. 1, 2020, pp. 1-14. doi: 10.11648/j.fm.20200601.11

Received: January 30, 2020; **Accepted**: February 11, 2020; **Published**: February 18, 2020

Abstract: This paper is directed at the important contribution to fluid dynamics made by Johan Nikuradze. His seminal paper published in 1933 represents the gold standard of empty conduit permeability, for the flow of water through roughened pipes, even to this very day. We revisit in some detail the "inflection profile" in Nikuradze's plot, which appears in the curve for his roughened data found in Figure 9 in that publication. In so doing, we show that the data points at low Reynolds number values, and particularly those surrounding the value of 3.4 approximately on the x-axis of his plot, do not represent the reported experimental results found in his tables of data. Furthermore, we also demonstrate that this discrepancy in his original paper is very problematic because it forms the basis for many subsequent scholarly works. As a result, this inflection profile has become erroneously embedded in conventional folklore concerning fluid flow in closed conduits and has enjoyed widespread acceptance as being a legitimate feature of fluid dynamics dogma. With the advent recently of Quinn's Law, a novel approach to the understanding of fluid flow in closed conduits, we are able to articulate in a manner not heretofore possible, the significance of this discrepancy which is far too important to ignore.

Keywords: Inflection Profile, Nikuradze, Friction Factor, Transition Region, Turbulent Flow, Wall Effect, Boundary Layer

1. Introduction

We begin by defining the problem in Nikuradze'z original publication [1].

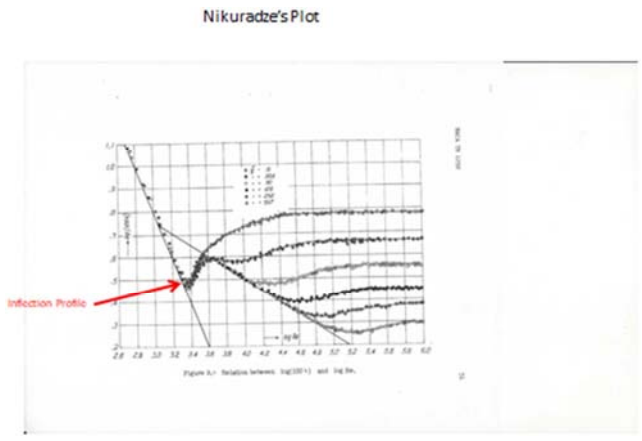

Figure 1. *Nikuradze's Plot.*

As shown in Figure 1 herein, which is a replica of Nikuradze's plot, there are many plotted points below a value of 3.6 on the x-axis. However, we cannot find anywhere in Nikuradze's paper any reported measurements in the tables of data which correspond to the plotted points below a value of 3.6 on the x-axis of his Figure 9. This is because in his tables of reported results, Nikuradze does not report any measurements below a Reynolds number of about 3,400. So the question to be asked is what does the plotted data points below a value of 3.6 on the x-axis represent, and what is the significance of the inflection point, if any, in the curve?

Our Analysis of Nikuradze's Figure 9.

On pages 10 and 11 of the paper, Nikuradze describes his plot in figure 9. In it he states "an extensive test program with a range of Re = 600 to Re = 10^6 for the Reynolds number was carried out, and the relationship of the resistance factor to the Reynolds number was studied for pipes of various roughness".

Although one would expect, then, to find experimental results at Reynolds number as low as 600, they are not reported in his tables 2 to 7. He does provide an explanation

for both the solid lines appearing in Figure 9 as follows; "as long as laminar flow exists, the resistance factor may be expressed as $\lambda = 64/Re$. This is represented in figure 9 by a straight line of slope 1:1", and again; "Within the first portion of turbulent flow in smooth pipes for a Reynolds number up to about $Re = 10^5$ the Blasius Resistance Law (reference 18) holds, $\lambda = 0.316/Re^{(1/4)}$. This is represented in the figure by a straight line of slope 1:4".

So we know that the straight line representing laminar flow is not generated as a result of his measurements, but rather represents theoretical dogma. In addition, the other straight line representing turbulent flow for smooth pipes was not created by his measurements either, but was taken directly from Blasius' theoretical equation. [2]

Next he describes the inflection point as follows; "The critical Reynolds number for all degrees of relative roughness occurs at about the same position as for the smooth pipe, that is, between 2160 and 2500". This range of Reynolds number corresponds to a range of values of 3.33 to 3.39 on the x-axis of figure 9, which identifies precisely the inflection point in the curve for the plotted data points that we cannot account for in his tables of reported data.

Thus, Nikuradze is, not only suggesting that there is a discrete value of the Reynolds number, which he terms the "critical Reynolds number" where laminar flow abruptly changes to transitional flow, but also that its value occurs between the Reynolds number values of 2,160 and 2,500.

2. Methods

Since we are challenging the inflection point in figure 9 in Nikuradze's paper, we need to perform our own experiments which cover the critical range of Reynolds number at issue in the transition region between the so-called laminar and turbulent region of his figure 9. In addition, we want to be able to validate the two theoretical lines drawn by Nikuradze, in order to bolster our challenge to the inflection point of his curve.

2.1. Experimental Setup

Our experimental apparatus was assembled as a prototype instrument designed for doing continuous flow chemistry. It consists of a fluid flow loop with calibrated pressure transducers for measuring pressure drop; several rtds along the pipe flow loop to monitor temperature at different locations; a circular gear pump to provide fluid flow up to a maximum of 200 psi; a computerized control system running Labview software manufactured by National Instruments; a spool of Teflon tubing having an internal diameter of 0.076 inches and three different lengths, 241 cm, 7,620 cm and 15,240 cm, the former was not coiled but used in a fully extended state. Large plastic reservoirs were filled with water at room temperature and the water was continuously recycled throughout the experiments. Graduated cylinders were used in conjunction with the stop watch in the computer to accurately measure the flow rate. The voltage of the power supply controlling the gear pump was set in the software, and for each flow rate measurement, the temperature and pressure drop across the Teflon tubing was recorded. We show three photographs of the experimental set up; Figure 2 is the fluidics module; Figure 3 is the spool of Teflon tubing; Figure 4 is the electronics module and computer control unit.

Figure 2. *Photograph of fluidics module.*

Figure 3. *Photograph of Teflon tubing.*

Figure 4. *Photograph of Electronics and computer control module.*

Table 1. *Teflon tubing measured results.*

L	Q		Temp	L	Q		Temp	L	Q		Temp
cm	mL/min	psi		cm	mL/min	psi		cm	mL/min	psi	
15,240	5	4.50	19	7,620	73	56	19	241	200	8	19
15,240	7	7.00	19	7,620	81	65	19	241	250	11	19
15,240	10	9.50	19	7,620	90	74	19	241	300	14	19
15,240	13	12.30	19	7,620	98	84	19	241	350	18	19
15,240	15	15.30	19	7,620	110	94	19	241	400	22	19
15,240	18	18.80	19	7,620	117	104	19	241	450	26	19
15,240	21	23.00	19	7,620	125	115	19	241	500	30	19
15,240	24	27.00	19	7,620	135	126	19	241	550	35	19
15,240	26	31.00	19	7,620	140	137	19	241	600	41	19
15,240	28	33.30	19	7,620	150	148	19	241	650	47	19
15,240	29	34.00	19	7,620	160	159	19	241	700	53	19
15,240	32	38.50	19	7,620	167	170	19	241	750	60	19
15,240	34	42.70	19	7,620	173	182	19	241	800	68	19
15,240	37	47.50	19					241	850	73	19
15,240	40	50.50	19								
15,240	42	54.50	19								
15,240	44	59.50	19								
15,240	47	65.20	19								
15,240	50	71.50	19								
15,240	52	74.00	19								
15,240	53	75.00	19								
15,240	58	85.00	19								
15,240	64	96.00	19								
15,240	69	108.00	19								
15,240	75	120.00	19								
15,240	80	132.00	19								

A total of approximately 50 separate measurements were taken and the results are tabulated in Table 1.

2.2. Experimental Results

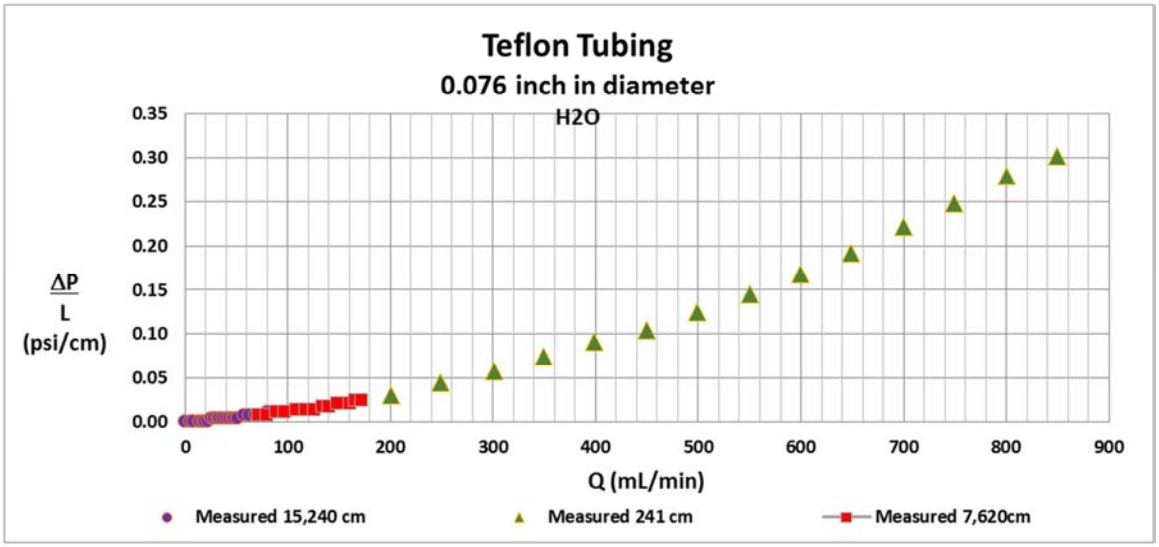

Figure 5. *Measured Permeability of Teflon tubing.*

As shown in Figure 5, we have captured our measured results for the Teflon tubing using three different lengths of that tubing, and plotted them as pressure gradient, ΔP/L, in units of psi/cm versus fluid flow rate, Q, in units of mL/min. It will be obvious from the plot that the lowest flow rates were achieved by the longest length of Teflon tubing. This is a result of the fact that we used a gear pump to generate our flow rate. It will be appreciated that gear pumps will deliver less flow rate at higher pressure drops. As can be seen from the plot, our flow rates varied between a low value of 5 mL/min and a high value of 850 mL/min. The corresponding range of total pressure drops measured was from a low of 4 to a high of 180 psi. This Teflon tubing is sufficiently rigid up to values of a total pressure drop of 200 psi to maintain the integrity of its diameter, i.e., below 200 psi the tubing diameter does not expand. In addition, the inner walls of the Teflon tube are extremely smooth, representing as it does probably the smoothest available material suitable for these

type of measurements.

We will now refer to the Quinn Fluid Flow Model (QFFM) to establish a correlation between our measured data and that implicit in Quinn's Law. [3]

We begin with equation (63) found in the publication.

This is the equation that relates the pressure gradient to other conduit parameters;

$$\frac{\Delta P}{L} = \frac{4\pi {r_h}^3 n_v}{3} + \frac{\delta \lambda n_k}{2\pi} \quad (1)$$

Where, $\Delta P/L$ = the pressure gradient; r_h = the normalization coefficient of fluid drag = 4; δ = porosity coefficient; λ = the fluid current wall-effect normalization coefficient; n_v = the viscous force per unit volume; n_k = the kinetic force per unit volume.

We note that the λ in the QFFM and Nikuradze's λ do not have the same meaning. Therefore, we will use in this paper the symbol with subscript λ_N to represent Nikuradze's λ to distinguish between the two.

Substituting for r_h in equation (1) gives;

$$\frac{\Delta P}{L} = \frac{4\pi 64 n_v}{3} + \frac{\delta \lambda n_k}{2\pi} \quad (2)$$

Simplifying equation (2) gives;

$$\frac{\Delta P}{4L} = 67 n_v + \frac{\delta \lambda n_k}{8\pi} \quad (3)$$

We can see from equation (3) that the pressure gradient term on the left hand side of equation (3) is the sum of a viscous and a kinetic term, both of which appear on the right hand side of equation (3). Normalizing for the viscous contributions, we divide across equation (3) by the term n_v. Thus we get;

$$\frac{\Delta P}{4Ln_v} = 67 + \frac{\delta \lambda R_{em}}{8\pi} \quad (4)$$

Where $R_{em} = n_k/n_v$

Rearranging equation (4) we get;

$$\frac{\Delta P}{4Ln_v} = 67 + \frac{\lambda Q_N}{8\pi} \quad (5)$$

Where $Q_N = \delta R_{em}$.

Rearranging equation (5) we get;

$$P_Q = 67 + \frac{C_Q}{8\pi} \quad (6)$$

Where $C_Q = \lambda Q_N$.

Finally, equation (6) may be written as;

$$P_Q = k_1 + k_2 C_Q \quad (7)$$

Where $k_1 = 64\pi/3 = 67$ (approx.) and $k_2 = 1/8\pi = 0.04$ (approx.)

Equation (7) is known as Quinn's Law of fluid dynamics.

We can see then that the term P_Q in the QFFM is a viscous type friction factor because it represents the measured pressure drop normalized for viscous contributions, and is a linear function of the term C_Q over the entire range of the modified Reynolds number which is an embedded term in C_Q.

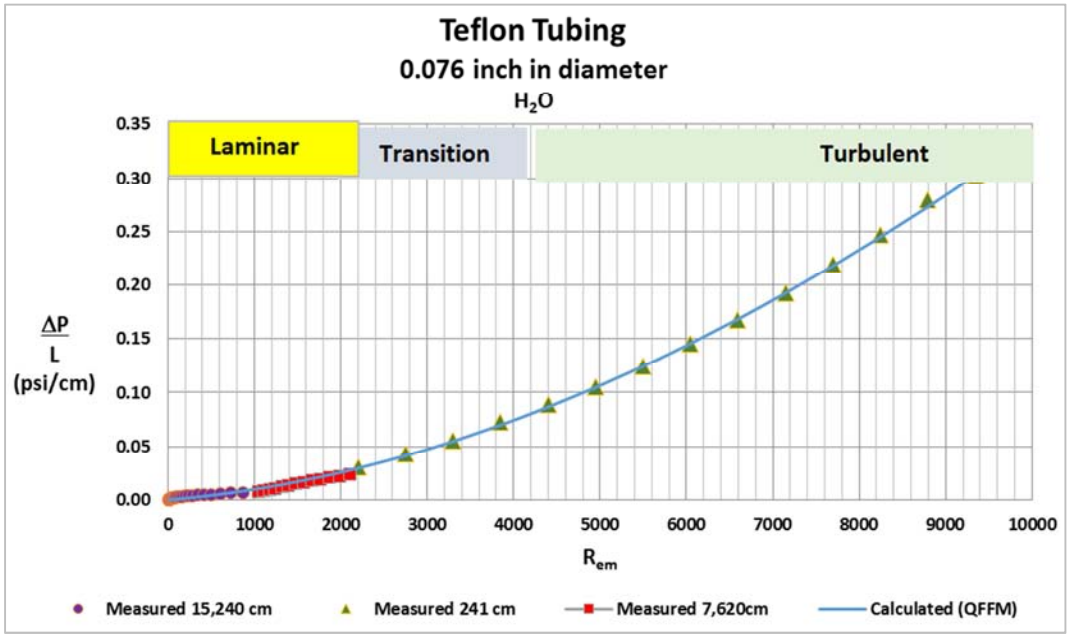

Figure 6. *Measured Permeability as function of R_{em}.*

In Figure 6 we show a plot of our measured results as a function of the modified Reynolds number as well as our calculated values based on the QFFM. Note the excellent correlation between the measured and calculated values. As can be seen in the plot, the flow rates used in the experiments correspond to a range of modified Reynolds number values from 10 to 10,000 and includes all three regions of the flow regime, i.e., laminar, transition and turbulent.

Next we present our measured result in the dimensionless form of Quinn's Law, i.e., after equation (6).

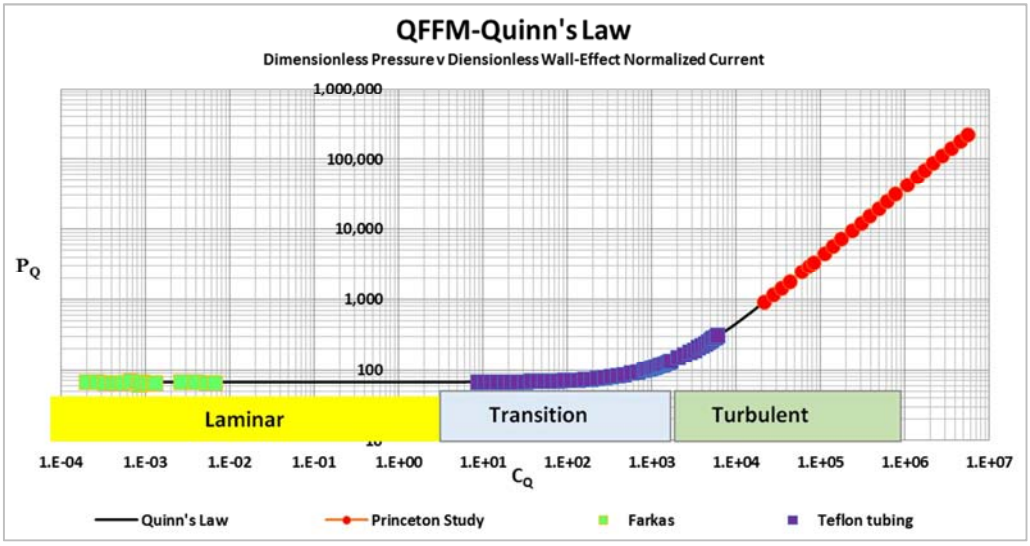

Figure 7. *Comparison of empirical results.*

In Figure 7 we show a plot of our measured results in the dimensionless parameters taught in the QFFM namely, viscous friction factor P_Q, versus wall-effect normalized fluid current C_Q. The plot is log-log and covers a range of Reynolds number values from 1×10^{-4} to 1×10^{7} which represents a range of 11 orders of magnitude. The plot describes a straight line of slope $1/8\pi = 0.04$ approximately, and intercept on the y-axis of $64\pi/3 = 67$ approximately. As a means of validating our measured results, we also show on the plot the third party published results of Farkas et al [4], the Princeton super-pipe study of McKeon et al [5, 6] and the line for smooth pipes according to the QFFM, i.e., Quinn's Law.

We emphasize that in Figure 7, we are exploiting one of the unique features of the QFFM which enables the comparison of data for packed and empty conduits on the same frame of reference. Thus, we include the packed conduit data from the paper by Farkas et al which enables us to validate the curve at extremely low values of the modified Reynolds number, i.e., creeping flow. This would not be possible using just an empty conduit because of measurement difficulties. We also point out that the modified Reynolds number is identical to the conventional Reynolds number in the case of empty conduits which is what we call a conduit that is not packed with particles.

As is obvious from Figure 7, our measured results for the Teflon tubing does not exhibit any non-linear behavior over the entire range of measured values.

2.3. Modeling our Results After Nikuradze

Next we present a comparison of our measured results to those presented in Nikuradze's figure 9 using the same frame of reference as Nikuradze.

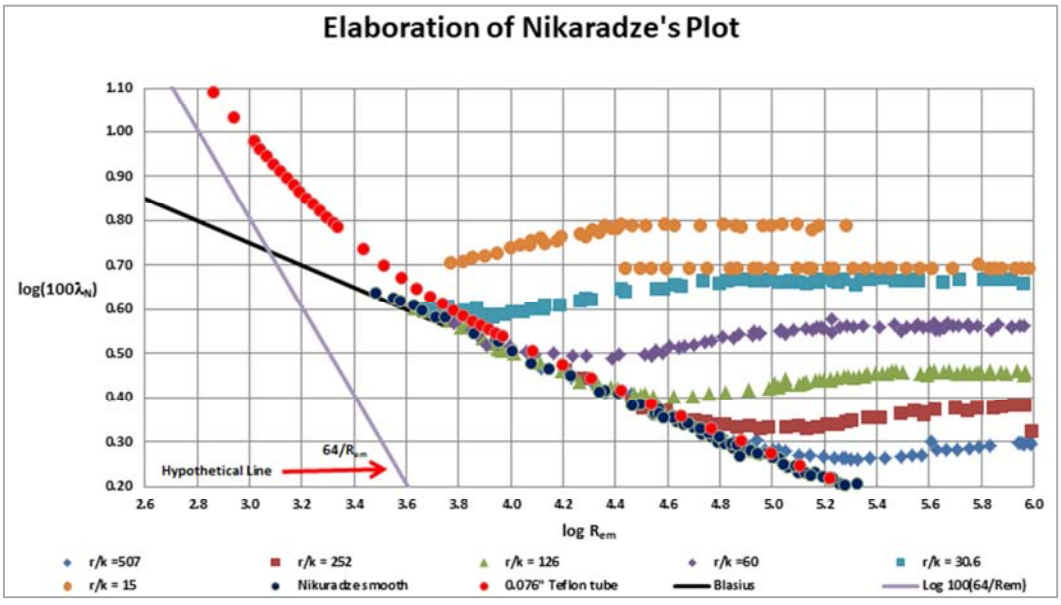

Figure 8. *Elaboration of Nikuradze's plot.*

As shown in Figure 8, we have made an elaboration of Nikuradze's plot in figure 9 of his original publication and we have included our measured data for the Teflon tubing as well as Nikuradze's data for smooth pipes from his original publication [7].

Firstly, note that there are no plotted data points for Nikuradze's data below a value of circa 3.5 on the x-axis and, accordingly, no inflection point at a value of 3.3-3.9 as stated in the text of his paper and shown in his figure 9.

Secondly, note that our measured data for the Teflon tubing extends to much lower values of the modified Reynolds number than that of Nikuradze's data, and includes the range of 3.3 to 3.39 on the x-axis which, according to Nikuradze, is where the inflection point in the curve is supposed to happen.

Thirdly, note that there is no inflection point in our measured data for the Teflon tubing.

It is also clear from Figure 8 that our measured data for the Teflon tubing makes a smooth transition between both the hypothetical line drawn by Nikuradze representing laminar flow and the Blasius dogma representing turbulent flow in smooth pipes, on the one hand, and Nikuradze's own measured results for roughened pipes, on the other hand. However, Nikuradze's plotted graph coordinates do not extend to low enough values of the modified Reynolds number to establish compatibility between our measured data for the Teflon tubing and his solid line for laminar flow. We therefore need to create an elaboration of Nikuradze's plot with coordinates extending to lower values of the modified Reynolds number to evaluate our measured data at much lower Reynolds number values.

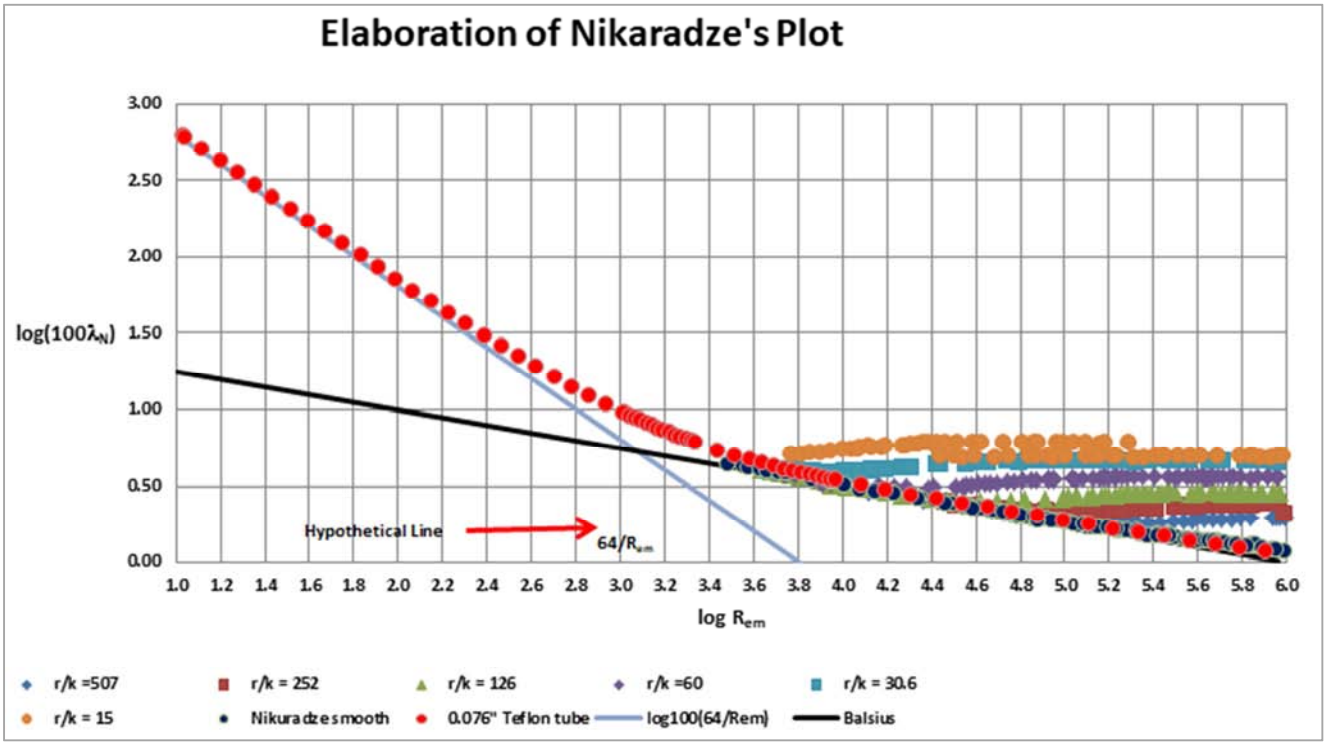

Figure 9. *Nikuradze's Plot coordinates expanded.*

In our Figure 9, we have extended Nikuradze's plotted graph coordinates down to a Reynolds number of 10. This corresponds to a value of 1 on the x-axis of this plot.

Note that close to a value of 1 on the x-axis of the plot, our measured values for the Teflon tubing fall on a line that is virtually identical to the line drawn by Nikuradze as representing that for laminar flow, i.e. his hypothetical line for $\lambda_N = 64/R_{em}$.

Finally, note that our measured data for the Teflon tubing demonstrates that there is a smooth transition between laminar and turbulent flow free of any abrupt rate of change and that, in particular, there is no inflection point visible in the vicinity of an x-axis value circa 3.3. In addition, we can see that our measured results for the Teflon tubing starts to deviate from Nikuradze's hypothetical line of $\lambda_N = 64/R_{em}$ representing laminar flow, at a value of the Reynolds number much lower than the values of 2,150 to 2,500.

Thus, not only does our measured data not show an inflection in the curve where Nikuradze asserts one to be, but it also demonstrates that the transition region of the flow regime starts at much lower Reynolds number values than suggested by Nikuradze.

2.4. The Significance of Nikuradze's Hypothetical Line for $\lambda_N = 64/R_{em}$

We now focus on the relevance of Nikuradze's hypothetical line for his laminar flow friction factor, i.e., $\lambda_N = 64/R_{em}$ and ask the rhetorical question, what does it represent?

To characterize the meaning of his $\lambda_N = 64/R_{em}$, we will first define its meaning in the terms of our QFFM. To do this, we start with our equation (5) above;

$$\frac{\Delta P}{4Ln_v} = 67 + \frac{\lambda Q_N}{8\pi}.$$

Nikuradze's friction factor λ_N is a kinetic type friction factor which distinguishes it from P_Q in Quinn's Law which, as we have shown above, is a viscous type friction factor.

Accordingly, we must normalize equation (5) for the kinetic contributions by dividing across by the term Q_N which gives;

$$\frac{P_Q}{Q_N} = \frac{k_1}{Q_N} + k_2\lambda \quad (8)$$

The left hand side of equation (8) is represented by P_K, the QFFM kinetic type friction factor. Thus we may write;

$$P_K = \frac{k_1}{Q_N} + k_2\lambda \quad (9)$$

Substituting for $k_1 = 67$ in equation (9), we get;

$$P_K = \frac{67}{Q_N} + k_2\lambda \quad (10)$$

We can see therefore that the term P_K in the QFFM is the equivalent of Nikuradze's λ_N, since they are both kinetic type friction factors.

We point out that equation (10) dictates that the kinetic type friction factor becomes infinite when the value of Q_N tends to zero, i.e., when the fluid is at rest. For this reason, the QFFM does not use this term but rather its reciprocal, which avoids this infinite boundary condition when the fluid is at rest. Thus, the term Θ is defined in the QFFM as;

$$\Theta = \frac{1}{P_K} \quad (11)$$

Where Θ = the dimensionless permeability, equivalent to the reciprocal of the kinetic friction factor.

It follows that we may write:

$$\Theta = \frac{1}{\frac{k_1}{Q_N} + k_2\lambda} \quad (12)$$

It further follows that we may now state that, in the limit, as the value of Q_N tends to infinity:

$$\lim_{Q_N \to \infty} \Theta = \frac{1}{k_2\lambda} = \frac{8\pi}{\lambda}.$$

Similarly, we may state that, in the limit, as Q_N tends to zero:

$$\lim_{Q_N \to \infty} \Theta = 0.$$

Accordingly, a plot of Θ versus Q_N will pass through the finite value of 0, when the fluid is at rest, and will approach the finite value of $8\pi/\lambda$ when the value of Q_N approaches infinity.

Nikuradze states that for laminar flow, his $\lambda_N = 64/R_{em}$ and he draws a straight line to represent this on his plot in Figure 9.

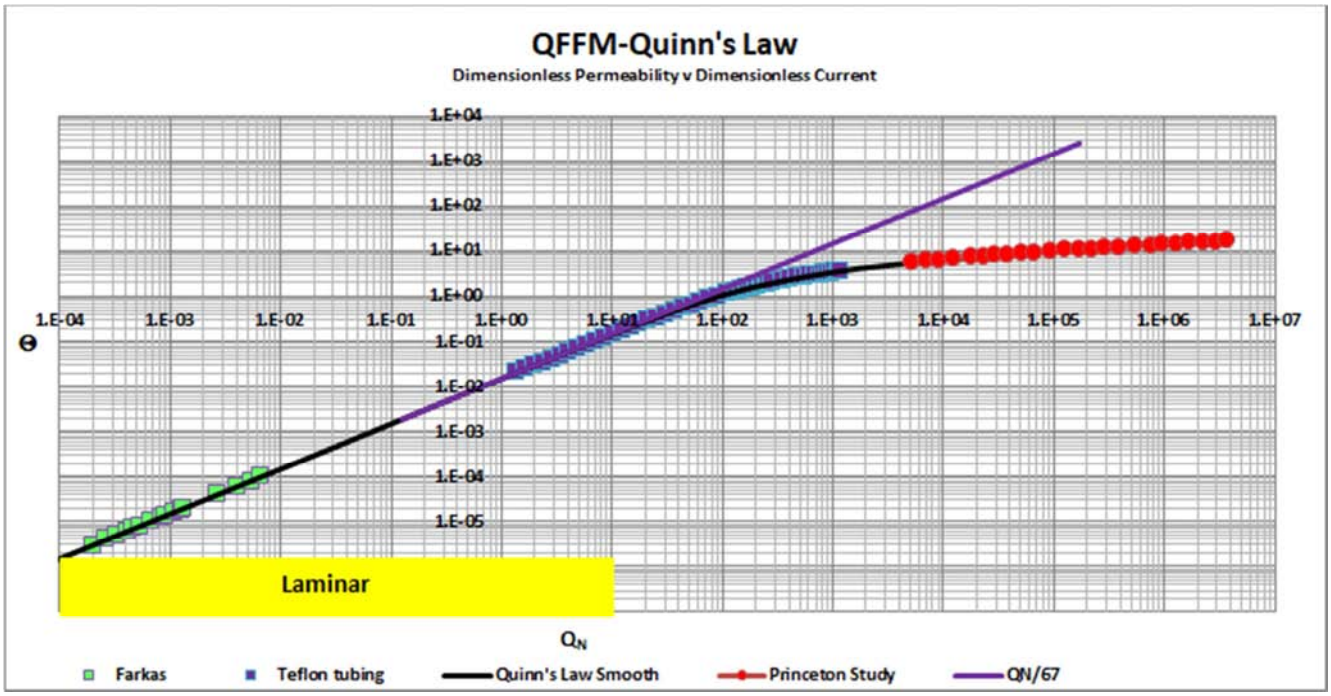

Figure 10. *Dimensionless Permeability.*

In our Figure 10, we have drawn a straight line for $Q_N/67$ which represents the reciprocal of our kinetic friction factor for laminar flow and corresponds to what Nikuradze did in his plot. We have to invert the term $67/Q_N$ to $Q_N/67$ in our plot to maintain parity with Nikuradze's methodology. As is obvious from Figure 9 herein, the straight line represented by $Q_N/67$ does indeed correspond to the regime of laminar flow.

It is clear now looking at both our figures 8 and 9 herein, that the QFFM and Nikuradze's fluid flow model are virtually identical for laminar flow, assuming we define laminar flow as being represented by a Reynolds number of circa 10, i.e., a value of about 1 on the x-axis of the plot in Figure 8.

There remains only the need to explain the difference

between the values of 64 in Nikuradze's laminar flow term and 67 in our laminar flow term. To articulate this difference we refer once again to the development underlying the QFFM beginning with our equation (1) above.

$$\frac{\Delta P}{L} = \frac{4\pi {r_h}^3 n_v}{3} + \frac{\delta \lambda n_k}{2\pi}$$

We now quote verbatim from the QFFM original paper.

Substituting for n_v and n_k in Equation (1), gives:

$$\frac{\Delta P}{L} = \frac{4\pi {r_h}^3 \delta \mu_s \eta}{3dc^2} + \frac{\delta^2 \lambda {\mu_s}^2 \rho_f}{dc} \quad (13)$$

Therefore, empirically, Equation (13) is the most useful equation for any practitioner. It demonstrates that when the fluid velocity, μ_s, tends to zero, (fluid at rest), and, therefore, the kinetic term (2nd term on right hand side of Equation (13)) is negligible, the *control volume element coefficient* is represented by $4\pi r_h^3/3 = 256\pi/3 = 268$ approx., since this is the multiplier in the viscous term of Equation (13) corresponding to the pressure gradient $\Delta P/L$. In other words, the *entire* control volume element is assigned to *viscous* considerations only, and is represented by the volume of a sphere having a radius r_h, the normalization coefficient of fluid drag. We can show this algebraically as follows (neglecting the kinetic term in Equation (1)):

$$\frac{\Delta P}{L} = \frac{4\pi {r_h}^3 n_v}{3} = 268 n_v \quad (14)$$

Equation (14) represents the empirically meaningful relationship between the *measured* pressure gradient (left hand side), and the fluid motion term (right hand side) when the fluid flow rate is very close to zero (laminar), i.e., kinetic contributions are negligible. Note that in this fluid flow regime, the fluid motion term is the product of two entities: n_v = the viscous hydraulic force exerted per unit element of fluid control volume and the constant value 268, ($4\pi r_h^3/3$ = 268), a/k/a the "viscous constant".

We can see then that the value of 67 is related to the so-called viscous constant in the Kozeny/Blake [8, 9] equation which is an equation that represents laminar flow in conduits packed with spherical particles. A value of 268 for that constant when normalized for fluid drag, i.e., when it is divided by $r_h = 4$, the normalization coefficient for fluid drag, gives the QFFM value of 67 [10-12].

Similarly, the value of 64 is related to the so-called viscous constant in the Poiseuille equation [13] which is an equation that represents laminar flow in empty conduits (no particles present). A value of 256 for that constant when divided by $r_h = 4$, the normalization coefficient for fluid drag, gives Nikuradze's value of 64.

Thus, we can see that this discrepancy between the values of 67 and 64 is less than 5% and in many experiments may fall under the radar due to experimental error [14].

2.5. Evaluation of the Blasius Relationship in Nikuradze's Plot

Next we turn our attention to the straight line drawn by Nikuradze which represents the Blasius friction factor for turbulent flow of smooth pipes.

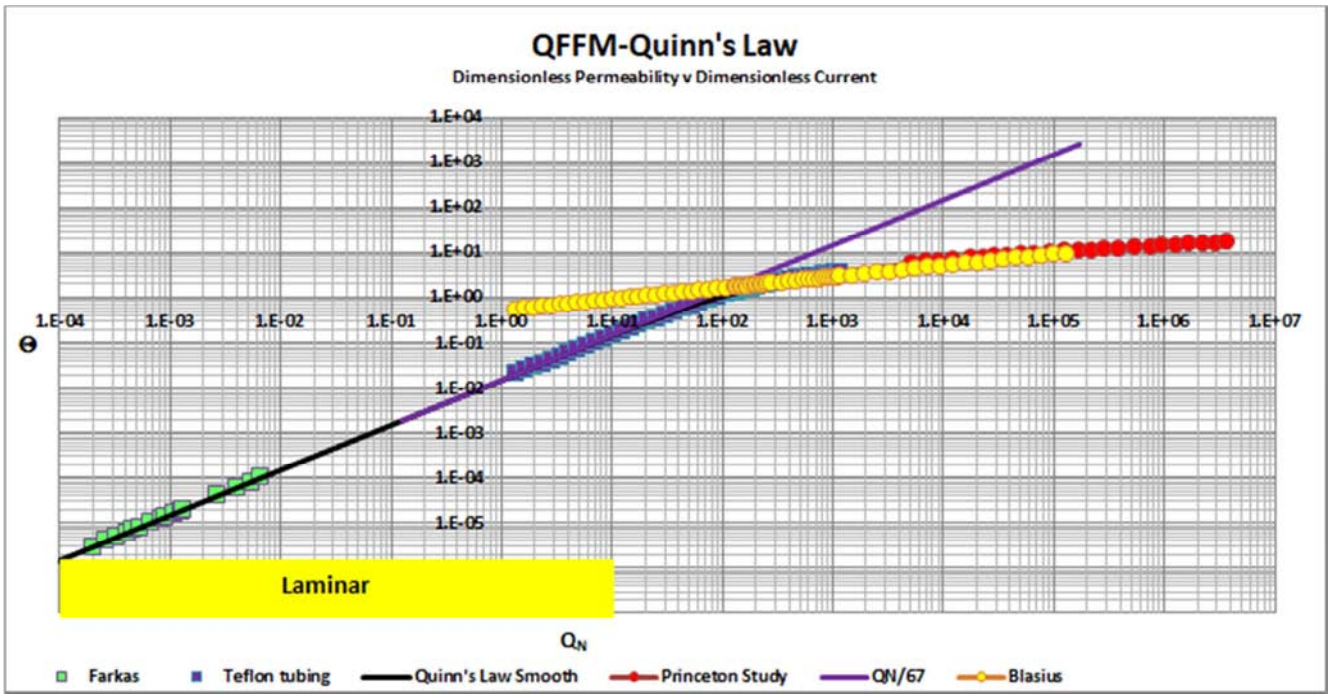

Figure 11. *Comparison of Dimensionless Permeability.*

In Figure 11 herein, we show where the Blasius line equivalent would appear in the QFFM plot. Note that it does indeed appear to correlate well with the results for smooth walled pipes in this frame of reference, i.e., a log-log plot over 11 orders of magnitude for the range of Reynolds number values.

2.6. Nikuradze's Data for the Roughened Pipes

Finally, we focus on Nikuradze's data for the roughened pipes in the turbulent zone.

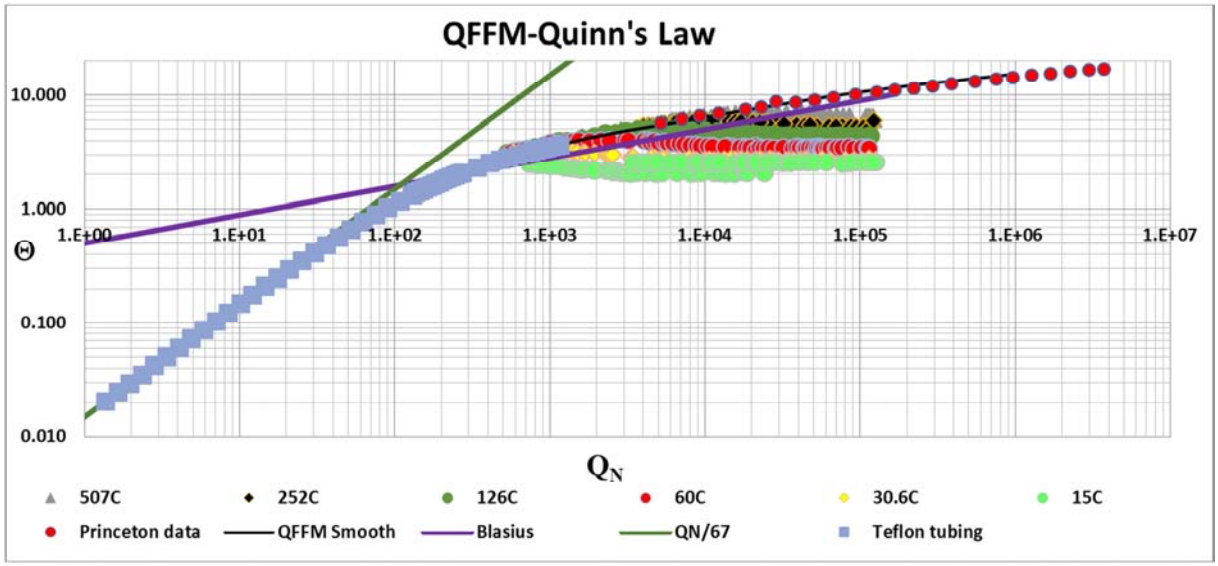

Figure 12. *Dimensionless Permeability of Roughened Data.*

In our Figure 12 herein, which is a plot of Quinn's Law, we include all the elements shown in Nikuradze's plot. All the elements show excellent correlation except that (a) there is no inflection point in the transition zone and, (b) the line representing the Blasius equation does not satisfactorily represent the true data for smooth pipes except at extremely high values of the Reynolds number and only there for a relatively narrow range of Reynolds number values, i.e., it intersects the true line rather than coinciding with it. This discrepancy between the Blasius equation line and the true line for smooth pipes is clearer in this plot because the coordinates of the plot are narrower and thus it provides a more sensitive analytical snap shot.

Finally, we can see that the lines representing Nikuradze's 6 degrees of relative roughness in the turbulent zone are nicely resolved and present a clear image of how roughness affects the kinetic friction factor. This plot highlights the genius of Nikuradze's roughened experiments.

3. Fluid Dynamic Anatomy of Nikuradze's Wall-Roughened Experiments

We have rationalized above, all the elements contained in figure 9 of Nikuradze's publication.

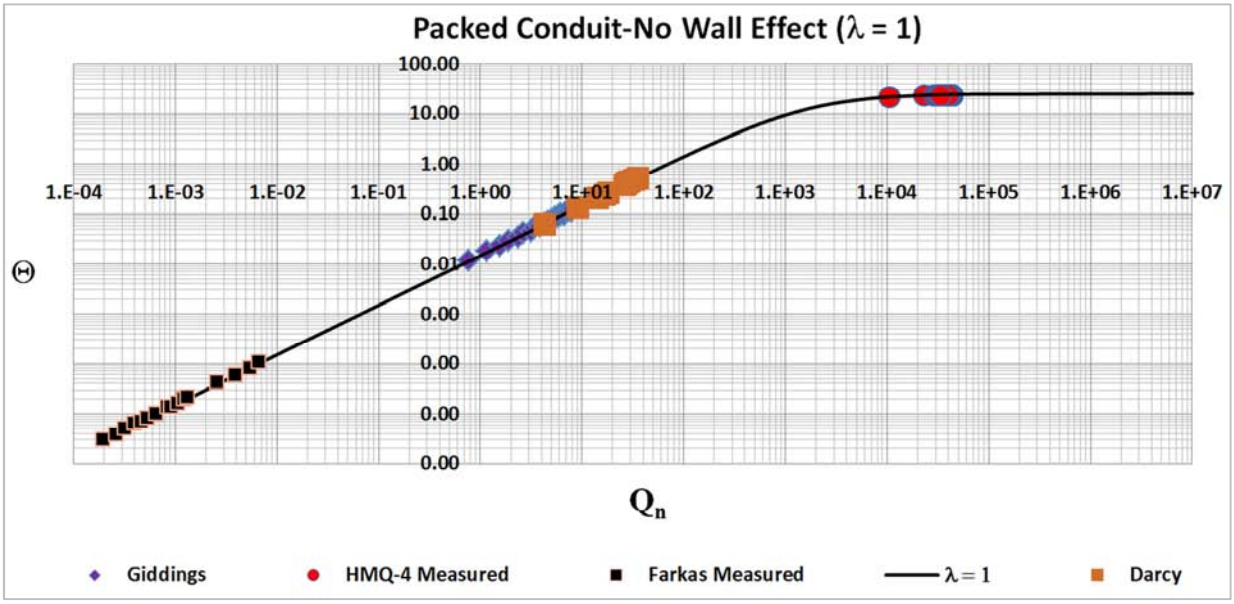

Figure 13. *Packed Conduits.*

We now drill down into his roughened experiments to fully explain their impact on the ramifications of fluid dynamics in closed conduits.

From a fluid dynamics perspective, Nikuradze's roughened wall experiments are all about the so-called "wall effect". After all, his experiments represent an ingenious methodology to graft roughness onto the inner wall surface of drawn brass pipes. This term, however, i.e., "wall effect", is a familiar topic in packed conduit jargon but, in empty conduit jargon, it is more often described in the context of the "wall boundary layer". We shall demonstrate below that both these concepts are one and the same in the eyes of the Laws of Nature and, accordingly, ought to be seamlessly absorbed in any unified theory of fluid dynamics.

3.1. No Wall-effect (λ = 1)

Before we get into what the implications of "wall effect" is in fluid dynamics, we need to understand what the *absence* of a wall-effect looks like, from a fluid dynamic perspective.

In Figure 13 herein, we show the teaching of Quinn's Law as it applies to packed conduits. In order to demonstrate the characteristics of packed conduits throughout the transitional and turbulent regions of the flow regime, we have included, in addition to the work of Farkas et al., which covers the creeping flow regime, the results of packed conduits from the published works of Giddings [15], Darcy [16] and Quinn [3]. As is evidenced from the plot, these results coincide perfectly with the line for λ = 1 in Quinn's Law. So we might ask, what is the relevance of λ = 1 in Quinn's Law?

To answer this question, we turn once again to the original publication of the QFFM in which we find the definition of λ at equation (44). We shall repeat that definition herein;

$$\Lambda = 1+W_N \tag{15}$$

Where, W_N = the net wall effect, and is restricted to where $0 \leq W_N$

The entity W_N is further defined as:

$$W_N = W_1+W_{2R} \tag{16}$$

Where, W_1 = the primary wall effect, W_{2R} = the residual secondary wall effect.

Thus, we can see from equations (15) and (16) that a value of λ = 1 means that there is no wall effect of any kind. We shall explain below the underlying reason for this assertion.

3.2. The Primary Wall Effect (W_1)-Smooth Pipe

Turning again to the original publication for Quinn's Law, we find the definition for W_1.

$$W_1 = \frac{\beta_0^{\frac{1}{3}}}{\tau} \tag{17}$$

Where, β_0 = the dimensionless boundary layer for a non-tortuous fluid flow and τ= the tortuosity coefficient for a given flow embodiment under study.

Thus, we can see that equation (17) establishes the relationship between W_1 the "primary" wall effect and β_0 the dimensionless boundary layer, in a closed conduit. We will not get into the mathematical definition of β_0 in this paper so that we can maintain our focus on the concepts rather than the detailed mathematics. (The reader can refer to the original publication of Quinn's Law to study at this level of detail).

Looking at equation (17), we can see that the primary wall effect W_1 is the dimensionless boundary layer for non-tortuous flow normalized for the tortuosity of the fluid flow embodiment under study, τ. But the value of τ for an empty conduit has the constant value of 0.188 (approx.) which is less than unity. (The reader can refer to the original publication of Quinn's Law to evaluate the definition of τ). In addition, for the special case of an empty conduit with smooth walls, wherein the residual secondary wall effect is equal to zero, we can see that the net wall effect $W_N = W_1$ [Equation (16)] and consequently the value of λ = (1+ W_1) and since W_1 is not equal to zero, the value of λ will be greater than 1.

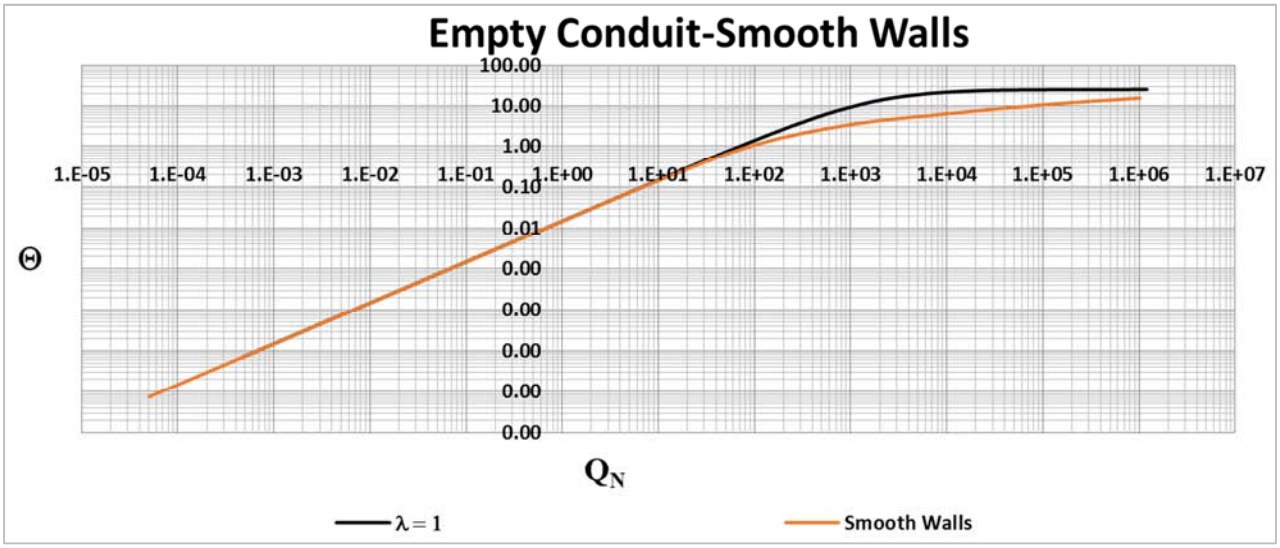

Figure 14. *Comparison of Empty and Packed Conduits.*

In Figure 14 herein, we show a comparison of the line for $\lambda = 1$ (packed conduit) and that for a smooth walled empty conduit. Note that at low values of the Q_N number there is no difference between the two. This is because in this laminar region of the flow regime, the kinetic term in the permeability equation is negligible and because λ manifests only in the kinetic term, it does not play a role in laminar flow. The difference is most pronounced in the transition region of the flow regime and diminishes as the flow becomes more turbulent. To evaluate this region of the flow regime, we will need to change the coordinates of our plot.

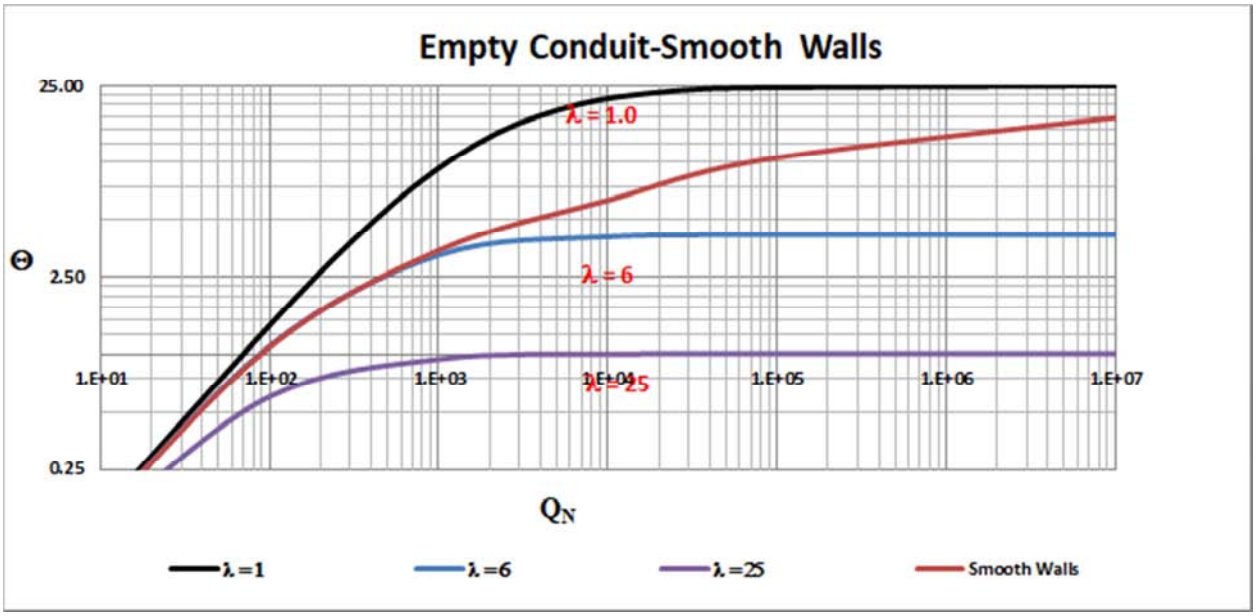

Figure 15. *Comparison of Dimensionless Permeability.*

In order to concentrate on the primary wall effect, which manifests only outside of laminar flow, we have narrowed the coordinates of our plot in Figure 15 to focus on Reynolds number values between 10 and 1×10^7 which includes both the transitional and fully turbulent regions of the flow regime. Note that the line for the smooth walled pipe has a maximum value for $\lambda = 6$ (approx.) at relatively low values of the Reynolds number but its value continuously decreases as a function of the Reynolds number approaching the λ value of 1 at extremely high values of the Reynolds number. This decreasing value of λ is due to the boundary layer being disrupted as the primary wall effect decreases at higher Reynolds number values due to increased turbulence. Accordingly, the primary wall effect is most pronounced at the onset of the transitional region of the fluid flow regime.

Now that we understand how the concept of the primary wall effect and the boundary layer are linked together in the case of a smooth walled pipe, it is an easy leap of faith to understand the underlying reason why the value of $\lambda=1$ for a packed conduit. The tortuosity coefficient of a packed conduit, τ, is typically enormous, i.e., many, many, many orders of magnitude greater than that in an empty conduit. Accordingly, the boundary layer is stretched over a much greater surface area which, in turn, reduces the thickness of the boundary layer, so that it is, in reality, infinitesimally thin, resulting in, no primary wall effect, no measurable boundary layer, and a value of $\lambda = 1$ which remains constant over the entire range of Reynolds number values. Thus, the distinguishing feature between a packed and an empty conduit with smooth walls is the tortuosity normalization coefficient, which is routed in the architectural make up of either flow embodiment. (Again we refer the reader to the original publication of Quinn's Law to study the definition underlying the tortuosity coefficient τ).

3.3. The Residual Secondary Wall effect (W_{2R})-Roughened Wall Conduit

Next we focus on the secondary wall effect which is due entirely to the roughness of the inner wall of an empty conduit. The roughness of the inner wall, characterized as "bumps" on the underlying smooth wall, will cause the fluid to change its trajectory, assuming that the bumps extend into the flowing fluid stream [17]. However, if the bumps are not large enough to "punch through" the boundary layer caused by the primary wall effect, they will have no net effect on the fluid trajectory. Thus, even though the bumps are present in all regions of the fluid flow regime, they will only manifest when they extend through the boundary layer. Accordingly, we call this extension beyond the boundary layer the "residual" secondary wall effect which means that the overall net wall effect, W_N, will be the sum of the primary wall effect and the residual secondary wall effect, which is evident from equation (16) herein.

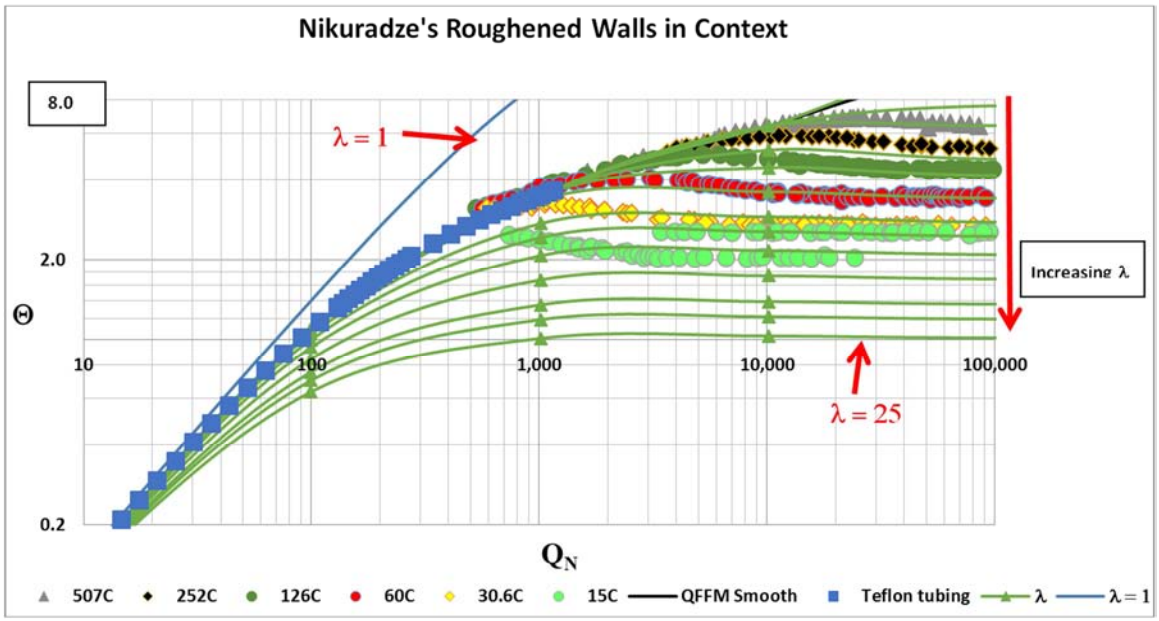

Figure 16. *Roughened Walls in context.*

As shown in Figure 16, the values for Θ corresponding to the values of λ reach a constant value at higher Reynolds number values.

Thus, Nikuradze's data show changing Θ values until the Reynolds number values become large enough, at which point they becomes constant. Thus, the "shoulder" that is evident in Nikuradze's data coming off the line representing smooth walls, is due to the ever decreasing primary wall effect as the Reynolds number values increase and it eventually disappears into a straight line when the primary wall effect is negligible and only the secondary wall effect remains, i.e. the residual secondary wall effect is equivalent to the total wall effect.

Accordingly, the only non-linear behavior exhibited in the kinetic friction factor of fluid flow in closed conduits, resides at Reynolds number values in the transition and near turbulent regions of the fluid flow regime and represents a gradual evolving profile rather than an abrupt profile change, and is due to the disappearance of the primary wall effect giving way to the secondary wall effect, as the Reynolds number values reach farther and farther into the turbulent region, i.e., the fluid flow profile becomes more and more turbulent.

4. Inflection Profile Based Scholarly Works

It is now almost 100 years since the inflection profile of Figure 9 of Nikuradze's publication became known to the scientific community and in that time period there are many scholarly attempts to validate Nikuradze's apparent inflection profile. We will now briefly review one of the most recent examples of this phenomenon to underscore the importance of this issue.

4.1. Worked Example (2018)

This is a very recent example of the proliferation of the Nikuradze inflection profile dogma, some 85 years after Nikuradze's original publication.

Unified Friction Formulation from Laminar to Fully Rough Turbulent Flow [19].

By Dejan Brkić and Pavel Praks.

Appl. Sci. 2018, *8* (11), 2036; https://doi.org/10.3390/app8112036.

Received: 14 September 2018 / Revised: 2 October 2018 / Accepted: 20 October 2018.

4.2. Author Abstract

"This paper gives a new unified formula for the Newtonian fluids valid for all pipe flow regimes from laminar to the fully rough turbulent. It includes laminar, unstable sharp jump from laminar to turbulent, and all types of the turbulent regimes: smooth turbulent regime, partial non-fully developed turbulent and fully developed rough turbulent regime. The formula follows the inflectional form of curves as suggested in Nikuradse's experiment rather than monotonic shape proposed by Colebrook and White. The composition of the proposed unified formula consists of switching functions and of the interchangeable formulas for laminar, smooth turbulent and fully rough turbulent flow. The proposed switching functions provide a smooth and a computationally cheap transition among hydraulic regimes. Thus, the here presented formulation represents a coherent hydraulic model suitable for engineering use. The model is compared to existing literature models, and shows smooth and computationally cheap transitions among hydraulic regimes.

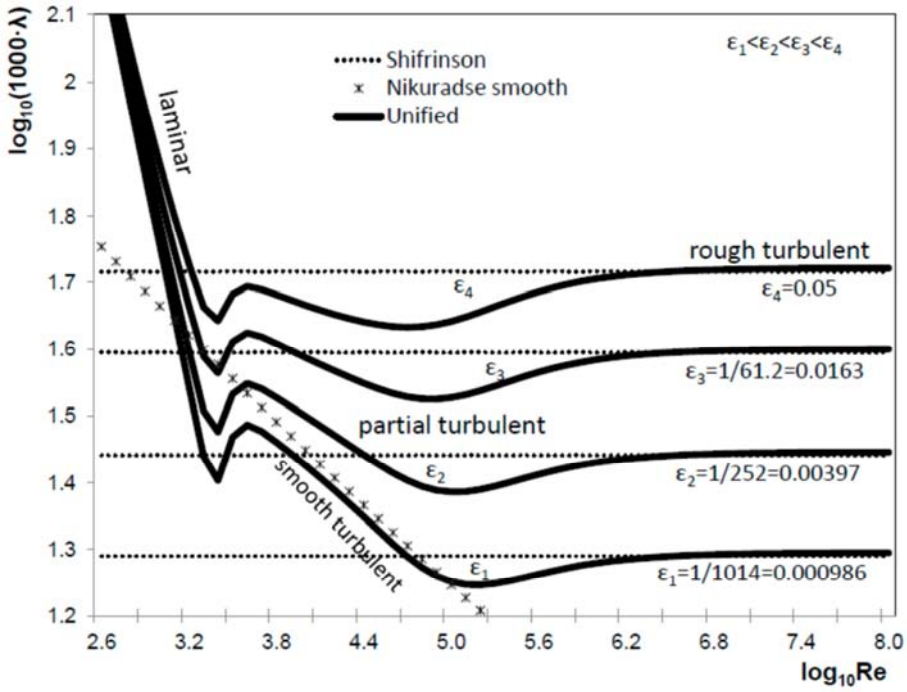

Figure 17. *The unified hydraulic model II; Equation (15).*

4.3. Author Conclusions

A sudden failure of valves or other components related to hydraulic systems in civil and mechanical engineering [35-37] can also cause a change of flow regime. Because of this, it is crucial to take such cases into consideration. The unified flow friction approach presented here is flexible, as proposed equations for a certain hydraulic flow regime can be easily altered using interchangeable formulas for laminar, smooth turbulent, and rough turbulent flow. Although our previous experiences with artificial intelligence [38-40] have shown that an encapsulation of all flow friction regimes into one coherent model is not a straightforward task, the form proposed here is simple. Thus, the unified approach presented here can be easily implemented with software codes. Moreover, as the proposed switching functions are carefully chosen so that they follow Nikuradse's inflectional law of roughness, our unified approach seems to be more realistic than the classic implicitly-given 80-year-old Colebrook–White monotonic curves model [41-46]. The switching functions presented here are expressed by simple rational functions and thus do not contain computationally expensive transcendental functions. Consequently, our unified flow friction formulation possesses a reasonable computational complexity."

We will not go into a lengthy analysis of this paper herein but we have included above, (a) the abstract, (b) the graph in Figure 15 containing the inflection profile and, (c) the conclusions, as direct quotes from the paper. These three extracts from the paper say all that needs to be said.

We make one final comment on this paper, however, which lies at the heart of this issue. We note that these authors did not put a scintilla of effort into designing and executing their own measurements of permeability in an empty closed conduit, to bolster their entirely mathematically driven development. Moreover, it is equally surprising that these authors did not put a scintilla of effort into mentioning their reasons for ignoring the fact that there exist no reported results in Nikuradze's tables of data that correspond to the so-called inflection profile.

5. Conclusions

In this paper we have raised serious questions concerning the inflection profile in Nikuradze's kinetic friction factor analysis surrounding his measurements of the permeability of water flows in the turbulent region, for his sand roughened pipes. Specifically, we have demonstrated that the plotted data points which define the inflection profile are not reported in his tables of data and, in addition, our measurements confirm that there is no inflection in the curve.

We have also provided our own measurements to bolster our challenge to the Nikuradze plot and by incorporating those measurements into the QFFM, we have established a unified frame of reference within which we compared Nikuradze's measurements to those of third party published results, such as those of the Princeton study in the super-pipe which covers a range of Reynolds number values within the fully developed turbulent regime, on the one hand, and the study by Farkas et al for packed conduits, which covers a range of Reynolds number values within the creeping flow and laminar region of the flow regime, on the other hand.

In addition, we have also demonstrated that the Blasius equation which is purported to provide an accurate projection of the friction factor for smooth pipes in the turbulent regime, is less than adequate, and can only be relied upon over a very narrow range of very high Reynolds number values within the fully developed turbulent flow regime.

Most importantly, regarding the region of laminar flow, we have shown that both our measurements and Nikuradze's measurements are virtually identical when viewed in the friction factor dimensionless analysis of either the QFFM or Nikuradze's own fluid model. This is an important result because it provides validation for the true value of the viscous constant which manifests in the Kozeny/Blake, Ergun and Poiseuille equations, a subject of much controversy for a very long time regarding the permeability of packed conduits.

In our evaluation of the experimental results of Nikuradze for roughened walls in the so-called turbulent regime, we have gone to great effort to explain how rough walls make a difference in the fluid dynamics of closed conduits. In so doing, we have used the underlying theory of Quinn's Law to demonstrate that the impact of wall roughness is all about the management of both the primary and the secondary wall effect. This explanation takes all the mystery out of some of the more bizarre accounts of boundary layer theory found in conventional dogma.

Finally, we have raised the issue of published scholarly works which do more damage than good because they derive theoretical relationships which are based solely on mathematically driven correlations without any grounding whatsoever in the Laws of Nature.

Declaration of Interests

The authors report no conflict of interest.

References

[1] Nikuradze, J. NACA TM 1292, Laws of Flow in Rough Pipes, July/August 1933. Translation of "Stromungsgesetze in rauhen Rohren." VDI-Forschungsheft 361. Beilage zu " Forschung auf dem Gebiete des Ingenieurwesens" Ausgabe B Band 4, July/August 1933.

[2] Blasius, H (1908). "Grenzschichten in Flüssigkeiten mit kleiner Reibung". Z. Angew. Math. Phys. 56: 1–37.

[3] Quinn, H. M. Quinn's Law of Fluid Dynamics Pressure-driven Fluid Flow Through Closed Conduits, Fluid Mechanics. Vol. 5, No. 2, 2019, pp. 39-71. doi: 10.11648/j.fm.20190502.12.

[4] Farkas, T., Zhong, G., Guiochon G.,, Validity of Darcy's Law at Low Flow Rates in Liquid Chromatography Journal of Chromatography A, 849, (1999) 35-43.

[5] Mckeon, B. J., Zagarola, M. V. and Smits A. J. A new friction factor relationship for fully developed pipe flow; J. Fluid Mech. (2004), vol. 511, pp. 41-44. Cambridge University Press; DO1; 10.1017/S0022112004009796.

[6] Mckeon, B. J., Swanson, C. J., Zagarola, M. V., Donnelly, R. J., and Smits, A. J., Friction factor for smooth pipe flow., J. Fluid Mech. (2005), vol. 238, pp. 429-443. Cambridge University Press; DO1; 10.1017/S0022112005005501.

[7] Nikuradze, J., NASA TT F-10, 359, Laws of Turbulent Flow in Smooth Pipes. Translated from "Gesetzmassigkeiten der turbulenten Stromung in glatten Rohren" VDI (Verein Deutsher Ingenieure)-Forschungsheft 356.

[8] Kozeny, J., "Uber kapillare Leitung des wassers in Boden," Sitzungsberichte der Kaiserlichen Akademie der Wissenschaften, vol. 136, 1927.

[9] Blake, F. E."The resistance of packing to fluid flow," Transactions of American Institute of Chemical Engineers, vol. 14, pp. 415-421, 1922.

[10] Quinn, H. M., A Reconciliation of Packed Column Permeability Data: Deconvoluting the Ergun Papers. Journal of Materials Volume 2014 (2014), Article ID 548482, 24 pages http://dx.doi.org/10.1155/2014/548482.

[11] Ergun, S. and Orning, A. A., Fluid Flow through Randomly Packed Columns and Fluidized Beds, Ind. Eng. Chem. vol. 41, pp. 1179, 1949.

[12] Ergun, S., Determination of Particle Density of Crushed Porous Solids, Anal. Chem. vol. 23, 1951.

[13] Ergun, S., Fluid Flow Through Packed Columns, Chem. Eng. Progr. vol. 48, pp. 89-94, 1952.

[14] Poiseuille, J. L. M., Memoires des Savants Etrangers, Vol. IX pp. 435-544, (1846); BRILLOUIN, M. (1930) Jean Leonard Marie Poiseuille. Journal of Rheology, 1, 345.

[15] Quinn, H. M., A Reconciliation of Packed Column Permeability Data: Column Permeability as a Function of Particle Porosity; Journal of Materials Volume 2014 (2014), Article ID 636507, 22 pages http://dx.doi.org/10.1155/2014/636507.

[16] Giddings, J. C., Dynamics of Chromatography, Part I: Principles and Theory, Marcel Dekker, New York, NY, USA, 1965.

[17] Brown, G., Henry Darcy and His Law, Biosystems and Agricultural Engineering, Ohlahome State University, 1999-2005.

[18] Prandtl, L. in Verhandlungen des dritten internationalen Mathematiker-Kongresses in Heidelberg 1904, A. Kraser, ed., Teubner, Leipzig, germany (1905), p. 484. English trans. In Early Developments of Modern Aerodynamics, J. A. K. Ackroid, B. P. Axcell, A. I. Ruban, eds., Butterworks-Heinemann.

[19] Brki´c, Dejan., and Praks Pavel,, Unified Friction Formulation from Laminar to Fully Rough Turbulent Flow; Appl. Sci. 2018, 8, 2036; doi: 10.3390/app8112036.